EPJ Web of Conferences **140**, 03059 (2017) DOI: 10.1051/epjconf/201714003059
Powders & Grains 2017

Experimental study of shear rate dependence in perpetually sheared granular matter

Sophie Yang Liu[1,⋆], *François* Guillard[1], *Benjy* Marks[1], *Pierre* Rognon[1,2], and *Itai* Einav[1,3,⋆⋆]

[1] *Particles and grains laboratory, school of Civil Engineering, The University of Sydney, Sydney, NSW 2006, Australia*
[2] *IUSTI-CNRS UMR 7343, Aix-Marseille University, 13453 Marseille, France*
[3] *Department of Civil, Environmental and Geomatic Engineering, Faculty of Engineering Science, University College London, London WCIE 6BT, United Kingdom*

Abstract. We study the shear behaviour of various granular materials by conducting novel perpetual simple shear experiments over four orders of magnitude of relatively low shear rates. The newly developed experimental apparatus employed is called "3D Stadium Shear Device" which is an extended version of the 2D Stadium Shear Device [1]. This device is able to provide a non-radial dependent perpetual shear flow and a nearly linear velocity profile between two oppositely moving shear walls. Using this device, we are able to test a large variety of granular materials. Here, we demonstrate the applicability of the device on glass beads (diameter 1 mm, 3 mm, and 14 mm) and rice. We particularly focus on studying these materials at very low inertial number I ranging from 10^{-6} to 10^{-2}. We find that, within this range of I, the friction coefficient μ of glass beads has no shear rate dependence. A particularly appealing observation comes from testing rice, where the attainment of critical state develops under much longer duration than in other materials. Initially during shear we find a value of μ similar to that found for glass beads, but with time this value decreases gradually towards the asymptotic critical state value. The reason, we believe, lies in the fact that rice grains are strongly elongated; hence the time to achieve the stable μ is primarily controlled by the time for particles to align themselves with respect to the shear walls. Furthermore, the initial packing conditions of samples also plays a role in the evolution of μ when the shear strain is small, but that impact will eventually be erased after sufficient shear strain.

1 Introduction

The mechanics of granular flow have been widely studied experimentally. Three flow regimes of granular materials include the quasi-static, inertial and collisional regimes [2], which are classified using the dimensionless Inertial number I [3]. It is defined as the ratio of the confinement timescale and the typical time of deformation [4, 5]: $I = \dot{\gamma} d \sqrt{\frac{\rho}{\sigma_{yy}}}$, where $\dot{\gamma}$ is the shear rate, σ_{yy} is the normal stress, d and ρ are the diameter and density of the grain respectively. This number is treated as the index of inertial effects in granular flows at various shear rates. Collisional rapid flows has been described by kinetic theories which provide a set of constitutive equations connecting the mean density, the mean velocity, and the granular temperature to the fluctuational energies induced by the binary collisions between particles [6]. The behaviour of the dense confined granular assemblies under extremely low shear rates are usually captured by an elasto-plastic, rate-independent constitutive law that characterises the critical state by the internal friction angle ϕ and the critical solid fraction v_c [7]. However, a comprehensive constitutive law is still lacking to fully capture the characteristics of granular flow in the intermediate inertial regime. Many studies [4, 5, 8, 9] have indicated a positive shear rate dependence of the friction coefficient μ, defined as shear stress over normal stress. In the study of da Cruz, et al. [5], the friction and dilatancy laws were proposed by conducting DEM simulation of 2D disc particles assembly in a plane shear configuration. It stated that the solid fraction v linearly decreases, but the friction coefficient μ linearly increases with the increasing I over 10^{-4} to 10^{-1}. However, Kuwano, et al. [10] carried out annular shear cell testing with 270μm diameter glass beads, and they reported a crossover from negative to positive shear rate dependence of the friction coefficient over the range of inertial number I from 10^{-6} to 1.

In this study, we employed a novel experimental apparatus called the "Stadium Shear Device" (SSD) that enables testing granular materials under perpetual shear conditions, here for the first time in three dimensions (i.e. 3D SSD). Unlike the Couette geometry which can only produce a radial dependent stress field, our new device is able to produce a non-radial dependent stress field in the central region[1]. We conducted perpetual shear tests on a large variety of materials, and present results examining the shear rate dependency of friction coefficient μ and the evolution of μ with shear strain.

⋆ e-mail: sophie.liu@sydney.edu.au
⋆⋆ e-mail: itai.einav@sdyney.edu.au

2 Experimental methodology

2.1 Introducing the 3D SSD

A schematic diagram of the 3D Stadium Shear Device is shown in Fig. 1(a). A belt customised from the belt designation Bando HTS 966-14M is centrally placed in a confining case (540 mm length ×250 mm width ×190 mm height). The belt has the same height as the confining case, and can be driven with shear rates in the range of $0.00645s^{-1} \sim 0.645s^{-1}$ from the power supplied by a motor and gear assembly installed on top of the driven sprocket. The granular material filled inside the belt is horizontally confined by two side plates of 175 mm length ×100 mm height, and vertically confined by a top and base plates as indicated in Fig. 1(a). Note that the sample has to be filled to a height above the side plate to accurately measure the normal stress using the two load cells (Mark-10 MR01-100#, one at front and one at back) attached on the side plates. Shear force is recorded by a torque transducer (Kistler 4520A050, range: 50 N.m) coaxially installed under the motor. There are 6 rows of 7 rollers bearings half-embedded on the surface of side plates to allow the belt run with minimal resistance. The friction between the running belt and the top plate are minimised using a brush-like draught excluder glued along the side of the top plate. In addition, the belt is sitting inside a U-shaped groove on the base plate with a Teflon sheet inserted to reduce the friction.

Fig. 1(b) schematically shows the stress state in the central confined region of the device, where σ_{zz} is the vertical normal stress applied through the top plate, and $\sigma_{yy} = \frac{F_N}{lh}$ the lateral stress, where F_N is the normal force measured by load cells, $l = 412$ mm is the projected longitudinal length of the belt and h ($h > 100$ mm) is the height of the sample. The in-plane shear stress $\tau_{xy} = \frac{S}{hp} = \frac{T}{rhp}$, where S is the shear force, T the torque applied by the motor and gear assembly, r the pitch radius of the sprocket, h the sample height and $p = 966$ mm the circumference of belt, respectively. The perpetual shear strain condition of the granular assembly within the belt is schematically illustrated in Fig. 1(c). Red thick arrows represent the directions of global shear direction and grey arrows indicate the localised shear directions within the sample. Due to the particular "stadium" shape of the belt, this device is able to perpetually shear particles and produce a continuous plane shear condition in the central region while re-circulating particles at either end without particle congestion. Although not shown here for brevity purposes, we used DEM, FEM and radiography studies to extract velocity profiles quite similar to the schematic one shown in Figure 1c.

2.2 Calibration procedure

A first calibration procedure was carried out to account for the forces induced by bending of the belt and frictions along interfaces between the metal plates and the belt. Before any experiment, the top plate was firstly kept at a certain height similar to the one it would have during the experiments (without material to be tested), and then the readings from both the load cells and the torque transducer were synchronously recorded when the belt was running at the velocity that would be operated during the experiment to be conducted later on. To avoid any possible hysteresis effects from the measuring meters, the same calibration procedure was repeated after every experiment. Since the calibration was made without the material, the forces measured were purely from the mechanical frictions mentioned above. The average force from two calibrations (before and after the experiment) was deducted from the corresponding shear and normal stresses during the experiments.

A second calibration procedure was conducted to examine the accuracy of the two load cells symmetrically attached to the adapt plates, which are connected to the side plates via bars on each side. This might lead to inaccurate readings of the normal force generated by shearing the sample. The calibration first involved tilting over the device in a horizontal direction, and then evenly placing over the side of the belt a bag of lead shot with known weight. This procedure was repeated many times with different weights. By comparing the readings of load cells with the actual weights, a factor of 1.71 with an error bar of 6% was adopted for the normal forces measured.

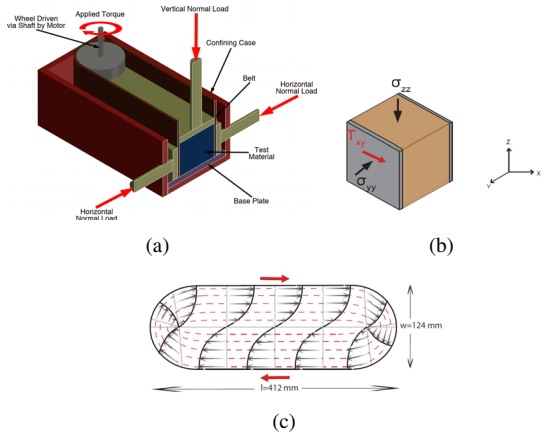

Figure 1. The 3D Stadium Shear Device (SSD). (a) An overview of the deive. (b) Schematic diagram of the granular assembly in the central region. (c) Schematics of velocity field. Red thick arrows show the global shear direction and grey thin arrows illustrate the flow.

2.3 Experimental procedure

In the present study, we tested glass beads with three different diameters (1 mm, 3 mm and 14 mm), for which the density of grain is roughly 2400 ± 100 kg/m^3 with less than 10% polydispersity. The mean aspect ratio (ratio between the smallest diameter and the largest diameter orthogonal to it) is 0.926. Another material tested was rice with a mean equivalent diameter of 3.8 mm and density of 1300 kg/m^2. The mean aspect ratio of the rice measured by macrophotographic imaging was 0.304, and the mean

circularity, defined as a function of perimeter P and area A, $\frac{4\pi A}{P^2}$ was found to be 0.542.

A set of tests with glass beads was conducted to investigate the relation between μ and inertial number I over the range of $10^{-6} \sim 10^{-2}$. The granular system was sheared to the same shear strain under different shear rates, and the normal and shear stress were measured only after the system achieved the critical state. Further discussion about the critical state is addressed in the results and discussions section. We firstly measured the shear and normal stresses under the lowest shear rate, and incrementally increased the shear rate to the highest possible. High reproducibility was indicated by repeating the same test from the highest shear rate to the lowest. The shear rate in our experiment is defined as velocity of the belt V divided by the width between two shearing walls w = 124 mm.

Furthermore, the evolution of μ with nominal shear strain $\epsilon = x/w$ (x being the distance travelled by the belt) was analysed with different particle shapes. In this test, the samples (3 mm glass beads and rice) were sheared to a shear strain of 240 at a constant shear rate with vertical stress σ_{zz} fixed. In addition, since the mechanical behaviour of a granular assembly is strongly dependent on its initial packing conditions, we compared the stress response and the critical states from dense and loose packed rice after more than 15000 shear strain. The loose sample was prepared by gently pouring a small amount of material into the device from minimal height until the target depth, while the dense one was prepared by compacting the sample layer by layer by hand.

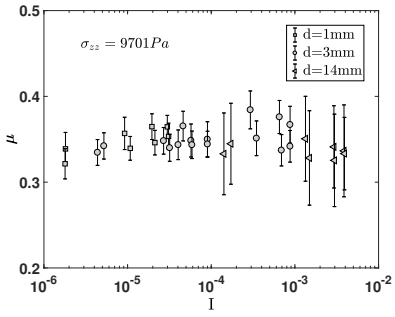

Figure 2. The shear rate dependence of friction coefficient μ for glass beads (initial void ratio is 0.645) with three diameters: 1 mm, 3 mm and 14 mm.

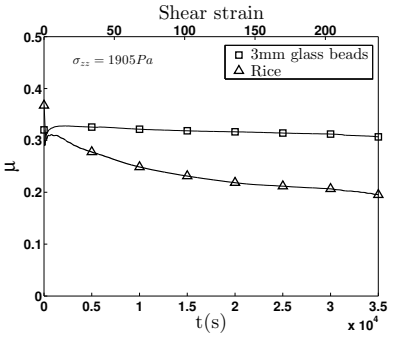

Figure 3. The friction coefficient μ over time and shear strain for shear rate of $0.00645s^{-1}$ on 3 mm glass beads and rice.

3 Results and discussions

In Fig. 2, the friction coefficient μ of glass beads at steady state is shown as a function of inertial number I over the range of $10^{-6} \sim 10^{-2}$. The low $I < 10^{-2}$ values correspond to granular flows in quasi-static regime. The symbols and error bars are the means and standard deviations of the stress readings over 10 belt turns, of which the accumulative shear strain is ϵ=79.2. By comparing the results from 14 mm glass beads with other smaller glass beads, one can find that the error bars are relatively large due to the smaller w/d ratio (w/d equal to 8.7, 40.7 and 122 for 14 mm, 3 mm and 1 mm glass beads respectively). The value of μ fluctuates slightly between $0.32 \sim 0.38$ and shows no dependence on the shear rate. This shear rate independence at the quasi-static regime is in agreement with previous studies. For example, da Cruz, et al. [11] and Iordanoff and Khonsari [12] identified shear rate independence in the quasi-static regime from discrete numerical simulations of 2D discs in a plane shear configuration, and the same characteristic was captured in [13] for polystyrene beads and glass beads in a Couette geometry. In particular, the value of μ from our experiments is very close to the μ_s that is an important parameter in the $\mu(I)$ rheology relationship [14]. This model assumes that the friction coefficient goes towards a minimum value μ_s at very low I, and μ_s is found to be equal to 0.38 for glass beads [15]. In [9], a weakly negative dependence of friction coefficient μ was found when $I < 10^{-3}$ and μ started increasing noticeably when $I > 10^{-2}$. However, no crossover from negative to positive shear rate dependence within this I range could be observed in our experiments. At this stage, we can not obtain data at I larger than 10^{-2} for glass beads because the velocity after solid-liquid transition is beyond the range covered by our device. In the future, further improvements will be implemented to increase the velocity range of the device.

To study the impact of particle shape on the friction coefficient μ, we compare μ as a function of shear strain for the tests of 3 mm glass beads and rice. As shown in Fig. 3, the rice exhibits a softening of friction coefficient with increasing shear strain, in contrast to the steady flow observed in glass beads. The value of μ decreases to two thirds of the initial value after shearing the rice to 240 shear strain. The same amount of friction coefficient reduction can be found in [16]. We believe that compared to spherical grains, elongated particles need a much longer shear duration to align themselves against the streamline, which increases the time to achieve the critical state. Further investigation into the alignment time and the orientation of the particles is out of the scope of the current paper.

The mechanical behaviour of a granular system is highly dependent on its initial preparation, and is expected to eventually reach a critical state that is independent of the initial packing conditions after sufficient shear strain [17]. In Fig. 4, we show the shear and normal stresses

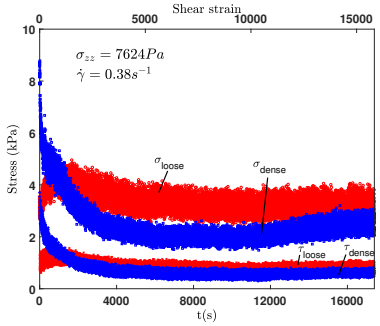

Figure 4. The normal and shear stress measured for dense and loose packed samples of rice.

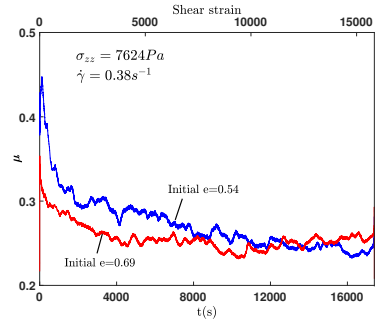

Figure 5. Friction coefficient μ over time and shear strain for the experiments shown in Fig.4. Note that the lines shown were smoothed over 160 s of data.

as a function of shear strain γ for both the initially dense (e=0.54) and loose (e=0.69) samples of rice. The samples are sheared at a shear rate of $0.38s^{-1}$ to a large deformation (15000 strain) with a constant vertical stress. The stress of the loose sample first reaches a peak at shear strain 600 before declining to a plateau at around 4000 shear strain, while the stress of the dense sample reduces from a higher initial value compared to the loose sample and may require more than 12000 shear strain to reach its critical state. Both systems converge to an identical value of 4 kPa for normal stress and 1 kPa for shear stress at the critical state. We also plot in Fig. 5 the friction coefficient μ as a function of shear strain and the same characteristics are observed: the value of μ converges to 0.25 after 16000 shear strain for dense system but only 4000 shear strain is required to reach the critical state for the loose one. Radjaï and Roux [7] also studied the critical state of initially dense and loose packed samples by conducting plane shear simulations with an assembly of rigid discs in two dimensions. Similar results were found in [7] except the peak of stress ratio was only observed in the dense packed system.

4 Conclusion

After conducting robust experiments with the 3D Stadium Shear Device, we found that the friction coefficient μ of glass beads is not dependent on the shear rate over four orders of magnitude at relatively low inertial numbers. The particle shape plays a role in the evolution of μ as a function of the shear strain. In particular, μ of granular assembly comprising elongated particles declines gradually to a plateau and reaches a critical state after very large deformation. By contrast, μ of spherical particles is fairly constant with increasing shear strain. The evolution of stress and μ at the beginning of shear is strongly influenced by the initial packing state but eventually collapse to the same value. Further research into the initial packing condition and its impacts on the stress responses and dilation curves will be an interesting topic to study. It would also be worthwhile to further examine (by numerical simulations) the properties of the device, for example, the shear strain condition and the stresses generated in the non-affine and rotational flows under the circular cap.

References

[1] T. Miller, P. Rognon, B. Metzger, I. Einav, Phys. Rev. Lett. **111**, 058002 (2013)
[2] C.S. Campbell, Journal of fluid mechanics **465**, 261 (2002)
[3] S.B. Savage, Advances in applied mechanics **24**, 289 (1984)
[4] G. MiDi, The European Physical Journal E **14**, 341 (2004)
[5] F. da Cruz, S. Emam, M. Prochnow, J.N. Roux, F. Chevoir, Physical Review E **72**, 021309 (2005)
[6] I. Goldhirsch, Annual review of fluid mechanics **35**, 267 (2003)
[7] F. Radjaï, S. Roux, The physics of granular media pp. 165–187 (2003)
[8] P. Jop, Y. Forterre, O. Pouliquen, Nature **441**, 727 (2006)
[9] T. Hatano, Physical Review E **75**, 060301 (2007)
[10] O. Kuwano, R. Ando, T. Hatano, Geophysical Research Letters **40**, 1295 (2013)
[11] F. Da Cruz, F. Chevoir, J. Roux, I. Iordanoff, Tribology series **43**, 53 (2003)
[12] I. Iordanoff, M. Khonsari, Journal of Tribology **126**, 137 (2004)
[13] F. Da Cruz, F. Chevoir, D. Bonn, P. Coussot, Physical Review E **66**, 051305 (2002)
[14] P. Jop, Y. Forterre, O. Pouliquen, Journal of Fluid Mechanics **541**, 167 (2005)
[15] Y. Forterre, O. Pouliquen, Journal of Fluid Mechanics **486**, 21 (2003)
[16] T. Börzsönyi, B. Szabó, G. Törös, S. Wegner, J. Török, E. Somfai, T. Bien, R. Stannarius, Phys. Rev. Lett. **108**, 228302 (2012)
[17] A. Schofield, P. Wroth (1968)